

Numerical Simulations of Flow past a 2-D Airfoil at a Low Reynolds Number

T. Ikeda, T. Kurotaki, T. Sumi, and S. Takagi

Japan Aerospace Exploration Agency (JAXA)

ABSTRACT

Karman-vortex shedding induced by wake instability behind a 2-D airfoil is of interest at relatively low Reynolds numbers, to understand how a vortex street develops in the wake region, and also how an aeolian tone is generated therefrom; this is supposed to show a different flow mechanism from a high-Reynolds number flow that exhibits more complicated viscous-flow phenomena. In this study, we performed numerical simulations of a 2-D laminar flow past an NACA0012 airfoil. The computation was run on the simulation code being developed to predict an aero-acoustic problems by using a highly accurate numerical method. For the verification of our code, the results are compared with the experimental data obtained in a similar flow configuration and also with an available numerical study. The detailed flow visualization is presented to understand the mechanism of the wake instability that results in vortex shedding.

Key Words: 2-D airfoil, wake instability, tonal noise

1. Introduction

We, Aerodynamics Research Group in JAXA, are now developing a computational fluid dynamics (CFD) code to simulate aeroacoustic phenomena at high accuracy. The code is designed primarily to perform a compressible large eddy simulation (LES) by combining high-order numerical schemes and an inverse filtering approach. As a prior study using this code¹, a high-Reynolds number flow past a two-dimensional airfoil was solved by successfully reproducing the boundary-layer transition after the occurrence of Tollmien-Schlichting instability waves. The study also captured the evidence of trailing-edge (TE) noise generation observed both in the sound pressure spectra near TE and the visualization of instantaneous pressure fluctuation.

However, it is also known that a tonal noise occurs in similar flow configurations at rather lower Reynolds numbers. In this case, a Karman vortex street develops in a laminar wake region, without the occurrence of direct emission of vortices from foil surface. Also, the difference should arise how the generated fluctuation of sound wave propagates in the boundary layer.

Our objective of this study is twofold. One is to understand the mechanism of vortex shedding and aeolian-tone generation, presumably induced by wake instability, at a low Reynolds number. The spatial and temporal dependence of velocity fluctuations are examined within both boundary layer and wake. Secondly, we would demonstrate the validation of our CFD code as an aeroacoustic solver: the detailed data of flow and generated sound levels are compared with other numerical and experimental studies^{2,3}.

2. Numerical Procedure

The description of numerical methodology is detailed in Ref. 1, including the derivation of modeling sub-grid scales (SGS) for LES. Since a laminar 2-D flow is expected at a low Reynolds number, we do not apply any SGS models and only 2-D components (streamwise and wall-normal directions) of flow variables are solved, although the code can treat general 3-D problems.

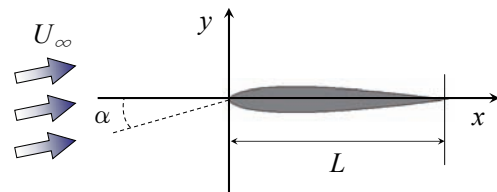


Fig. 1 Flow configuration

A schematic view of geometrical configurations is shown in Fig. 1. NACA0012 airfoil of the chord length L is aligned to the x -axis, so that the origin of coordinates comes to the leading edge. The Reynolds number based on L and the inflow velocity U_∞ is 7500, and the inflow Mach number is 0.1. The angle of attack α varies from 0.0 to 5.0[deg.] in this study. Flow field is discretized using C-grid topology with an interface condition applied where two boundaries collapse from TE toward downstream in the wake region. The grid dimension of the results shown here is $900 \times 160 = 144,000$, which is relatively small to be used in a direct simulation of aeroacoustics; for instance, nearly 2 million grid nodes were used at

Re=5000 in Ref. 2. However, the grid convergence is confirmed so that near-field sound pressure levels would not be affected by insufficient resolution.

3. Wake Instability

First, the instantaneous streamwise velocity (or u -velocity) contours are shown, from the middle of the airfoil to $2L$ downstream from TE, and compared for three different angles of attack, in Fig. 2. With no incident angle, almost no unsteady motion can be recognized just behind the airfoil; the vortex shedding gradually develops in the wake, and the velocity fluctuation takes its maximum at about $x=2L$, one chord length down from TE. Fig. 3 shows the power spectrum density (PSD) of wall-normal velocity (or v -velocity) at the location. The primary shedding frequency obtained for $\alpha=0.0[\text{deg.}]$ is 2.2, while those reported in Refs. 2 and 3 are close to ours, 1.8 and 2.5, respectively. As α increases, the location of the maximum u -fluctuation shifts toward upstream. At $\alpha=5.0[\text{deg.}]$, a considerable recirculation zone forms on the suction side near TE; vortices are directly generated therefrom, which resembles the vortex shedding of a bluff body.

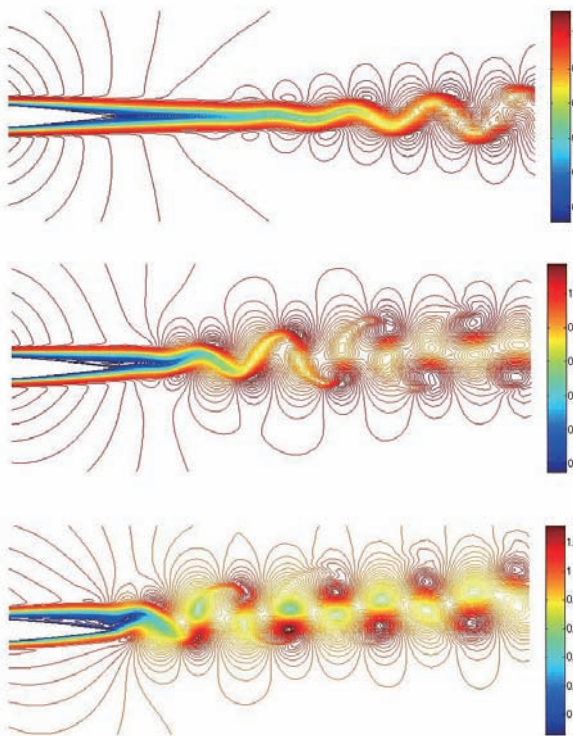


Fig. 2 The development of Karman vortex street: (top) $\alpha=0.0$; (middle) $\alpha=2.5$; (bottom) $\alpha=5.0[\text{deg.}]$.

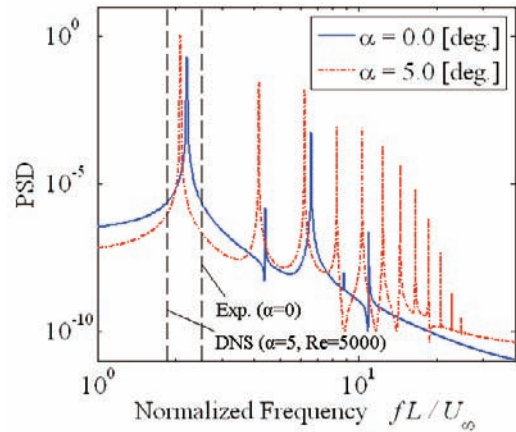


Fig. 3 PSD of v -velocity at $x=2L$

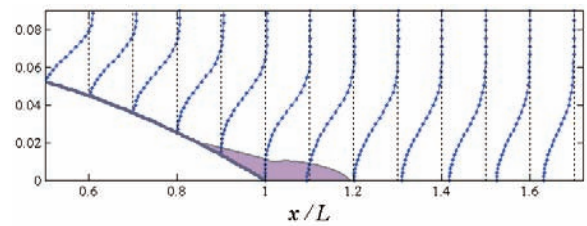


Fig. 4 Streamwise velocity profiles near TE ($\alpha=0.0$). Filled region indicates reverse flow.

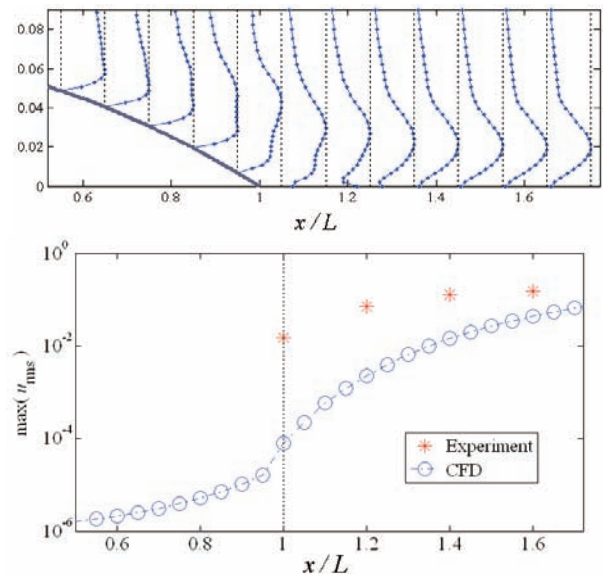


Fig. 5 RMS u -fluctuation ($\alpha=0.0$): (top) normalized profiles; (bottom) growth of maxima.

By examining the time-averaged velocity field for $\alpha=0.0[\text{deg.}]$ in Fig. 4, a bell-shaped profile is obtained in the wake. Clearly, the self-excited vortex shedding is attributed to the inflexion-point instability. However, we also see a reverse flow region around TE. It is possible that the growth of fluctuation, after the boundary layer separates, could be increased abruptly by the presence of reverse flow, as seen in Fig. 5. In the same diagram, the

experimental data of Ref. 3 are shown. The discrepancy may be explained by the wind-tunnel inflow fluctuation, as well as measurement errors. Also, the experimental peak location of maximum is rather close to TE than our numerical result; inflow fluctuation may accelerate the development of the Karman vortex. However, the overall maximum of u -fluctuation agrees well in both cases, as their maxima collapse toward downstream.

4. Tonal Noise Generation

Even though vortices are not fully developed near TE, as portrayed in Fig. 2, still an aeolian tone is generated by the interaction between the foil-surface and vortex shedding, unlike a bluff body case. Fig. 6 shows the generation and propagation of sound pressure up to about $10L$ from the airfoil. Our simulation code clearly reproduces fairly weak pressure fluctuation. Fig. 7 is the close views of a sound source. As shown in the figure of $\alpha=0.0$ [deg.], the undisturbed pressure oscillation indicates that the pressure fluctuations in the wake do not necessarily represent the presence of vortices traveling with them, since the vortices form rather downstream.

The magnitude of sound wave at $1L$ vertically away from TE is of the order of as low as 10^{-7} for $\alpha=0.0$, but still consistent with the other two cases, as well as the results in Ref. 2: dipole sound is generated near TE with the frequency of vortex shedding, and decays with $r^{-1/2}$ dependence, as shown in Fig. 8 by dashed line. As also seen, the sound pressure level strongly depends on the angle of attack, α . The increase of α enlarges the cross-sectional area for the inflow, which practically increase the Reynolds number. However, also with the increase of α , the separation bubble at TE becomes more distinguishable, which energizes vortex shedding, and eventually sound generation, too.

Fig. 8 also shows sound pressure levels at $\alpha=5.0$ [deg.] in Ref. 2. The reference cases were run at a different Mach number, 0.2; the plotted data were modified for $M=0.1$ by the factor $M^{2.5}$, Mach number dependence of 2-D dipole sound. The remaining discrepancy is due to the Reynolds number difference. We also tested the case of $Re=5000$ and $\alpha=5.0$ [deg.] on our code and obtained results well-agreed with Ref. 2; they are not shown here.

As for the velocity fluctuation due to the sound wave, Fig. 5 shows the positive growth of u -fluctuation all the way from the middle of the chord. However, the growth rate is altered abruptly across TE, which implies the different mechanism to amplify velocity fluctuations. To examine this, u -velocity is monitored in several locations in the boundary layer, as shown in Fig. 9. The sinusoidal temporal variations at all the locations do not exhibit a significant phase difference. In addition, the

instantaneous u -fluctuation contours do not show any discernible phase distribution in the streamwise direction, although the amplitude of fluctuation does show the exponential dependence as was shown in Fig. 5. This observation suggests that the fluctuations in the boundary layer represent a linear disturbance of acoustic wave decaying toward the leading edge, not the unsteady motions transmitted from an upstream region. Therefore, at this low Reynolds number, acoustic disturbance does not affect the laminar boundary layer on airfoil surface.

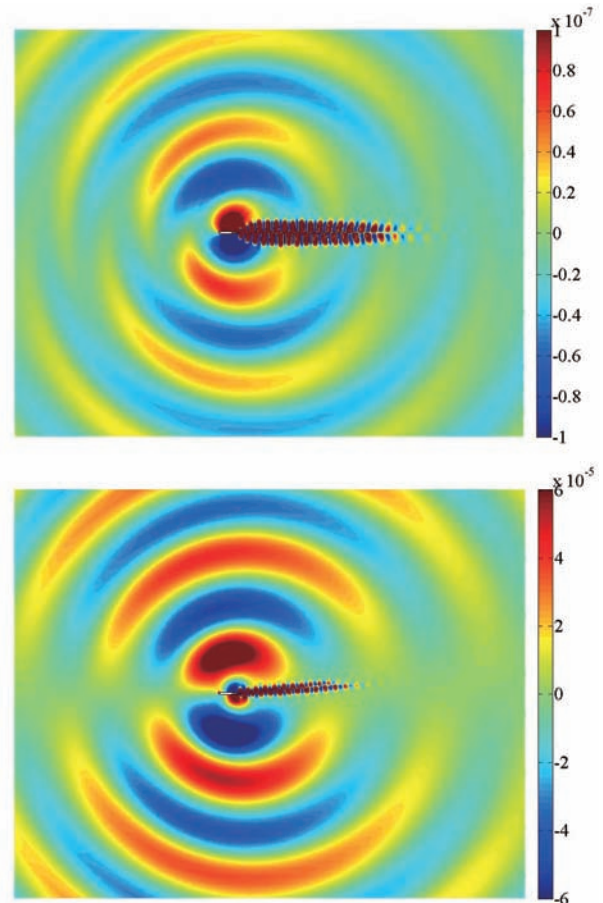


Fig. 6 Instantaneous pressure fluctuation: (top) $\alpha=0.0$; (bottom) $\alpha=5.0$

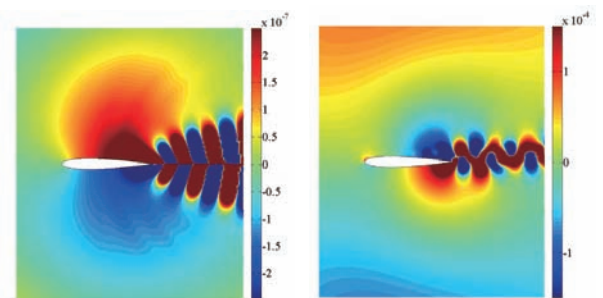


Fig. 7 Close views of instantaneous pressure fluctuation: (left) $\alpha=0.0$; (right) $\alpha=5.0$

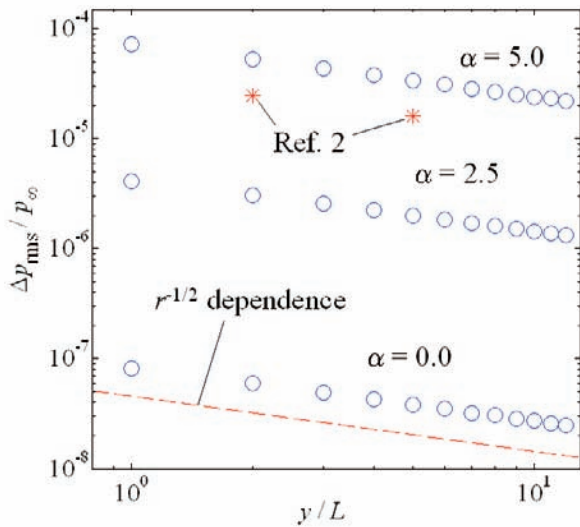


Fig. 8 RMS pressure fluctuations decaying on the distance from TE: \circ , current simulations; $*$, Ref. 2 (Re=5000, $\alpha=5.0$)

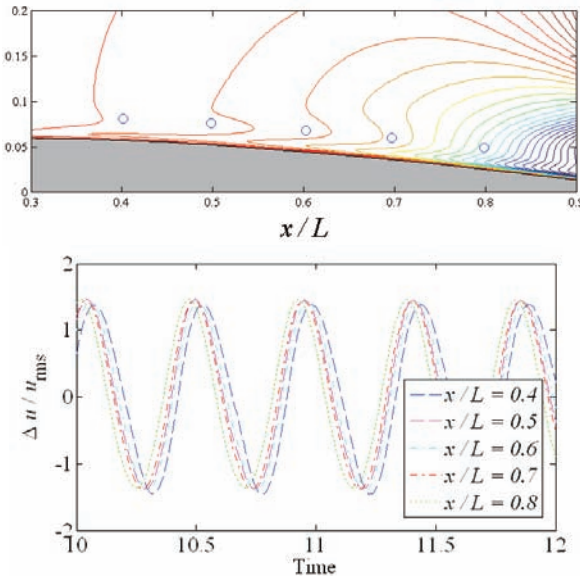


Fig. 9 Phase difference in boundary layer: (top) instantaneous u -fluctuation contours and monitoring locations denoted by \circ ; (bottom) time history of u -fluctuation normalized by its RMS.

5. Summary

The two dimensional wake instability of flow past NACA0012 at Re=7500 was successfully reproduced by our simulation code that is being developed to solve aero-acoustic problems. A quantitative examination of velocity distributions and fluctuations, as well as shedding frequencies achieved a sufficient agreement with other studies. Visualizations also depict the qualitative mechanism of vortex-shedding development.

Aeolian tones, portrayed well in the instantaneous pressure fluctuation fields, also provide quantitatively accurate behavior. Unlike bluff body flows, pressure fluctuation moving downstream in the wake is not directly associated with vortices, although the frequencies of both pressure fluctuation and vortex shedding are consistent. Nevertheless, a dipole sound is produced at the vicinity of TE through the interaction of the airfoil surface and the Karman vortex that develops away from the foil.

On the boundary layer receptivity, we observed no evidence that the sound wave affects the boundary layer. The linear wave is only transmitted toward upstream from TE, and decays very quickly. The Karman vortex develops in self-exciting mechanism induced by the instability of wake velocity profiles, not affected by acoustic disturbances.

References

- 1) T. Kurotaki, T. Sumi, and T. Atobe: Numerical simulation around airfoil with high resolution in high Reynolds numbers, AIAA Paper 2007-720
- 2) T. Irie, N. Hatakeyama, and O. Inoue: Direct numerical simulation of aerodynamic noise around an airfoil, *Proceedings of 8th Japan-Russia CFD Symposium*. (2003), P.14-15
- 3) S. Takagi, T. Kamono, and S. Rikitake: Wake instability behind and NACA0012 at low Reynolds numbers, *Proceedings of 6th International Symposium on Advanced Fluid Information* (2006), P.91-92